Novel FF Control Algorithm of Robot Arm Based on Bi-articular Muscle Principle - Emulation of Muscular Viscoelasticity for Disturbance Suppression and Path Tracking -

Kengo Yoshida[1], Toshiyuki Uchida[1], Yoichi Hori[1]
[1]Department of Electrical Engineering University of Tokyo
4-6-1 Komaba, Meguro Tokyo153-8505, Japan
yoshida@horilab.iis.u-tokyo.ac.jp, uchida@hori.t.u-tokyo.ac.jp, hori@iis.u-tokyo.ac.jp

Abstract— **Recently there are many trials to introduce animal characteristics into robots. Animals have amazing control ability. We consider that muscular viscoelasticity and muscular arrangements have important roles in such ability.**

In this paper muscular arrangements of upper arm are simplified to a model consist of four mono-articular muscles and two bi-articular muscles. We suggest novel control method to drive this simple arm model with feedforward control. This method obtain robustness like feedback control to use muscular viscoelasticity.

Furthermore we made an robotarm based on the principle of bi-articular muscles to verify proposed method. Its mechanism and control method is described.

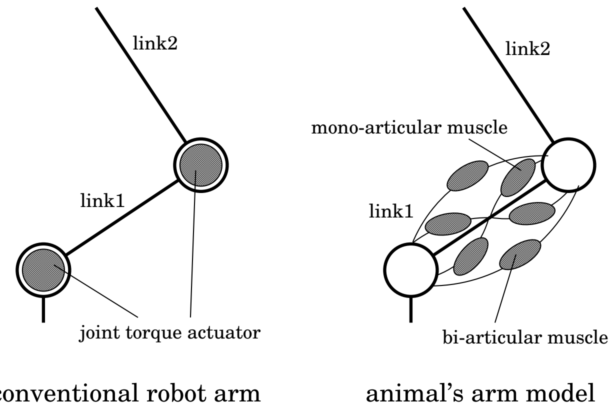

Fig. 1. Conventional robot arm model and animal‘s arm model

I. Introduction

Today, many robots which have animal-like appearance are researched and developed, and they can imitate animal movements. However they don‘t imitate animal‘s actuators and control mechanisms.

Conventional robots have actuators which drive only one joint, and usually rotational electromagnetic motor are installed in each joint. On the other hand, animals has muscles to move their body. Muscle is a kind of linear actuator which has unique viscoelasticity. They has complex muscular arrangements. Some muscles can drive two or more joints. Fig. 1 shows simplified conventional robot arm model and animal‘s arm model.

For control mechanisms, both conventional robots and animals mainly use feedfoward control. Computed torque method is one of popular mechanisms to control conventional robots. It needs vast calculation amount and precise model of robots and environments. Robots can move very fast and precisely in known and stable environments. However they easily get unstable by small disturbances.

Animals has robustness for various environments and disturbances. Therefore, animals must have some mechanisms similar to feedback control. Animals receive many informations from eyes, semicircular canal and so on, but they must not feedback these informations directly and immediately. Because it takes very long time to reach these informations to distal locomotorium. We consider that animals use muscular viscoelasticity as feedback mechanism, and unique muscular arrangement may give some effect to control mechanisms.

In this paper, Novel feedforward control algorithm of robot arm based on bi-articular muscle principle is proposed. Muscular viscoelasticity and muscular arrangement contribute to disturbance suppression and path tracking. We simulate this algorithm and verify its effectiveness. Finally an robot arm which we made for experiments is introduced. we described its mechanism and control diagram.

The following are earlier study about bi-articular muscle and muscular viscoelasiticity. Van Ingen Schenau et. al. described a role of bi-articular muscles in vertical jump. Gastrocnemius muscle which is a bi-articular muscles in the calf of the leg develops and transmits propulsive force.[1]

Neville Hogan suggested that antagonistic bi-articular muscles can control mechanical impedance. And he showed its effectiveness at contact tasks. [2][3]

Mussa-Ivaldi ascertained changes of a stiffness ellipse at the end point of human arms by changing arm postures through experiments. [4]

Kumamoto and Oshima et. al. suggested modeling of human arms and legs using two antagonistic pairs of mono-

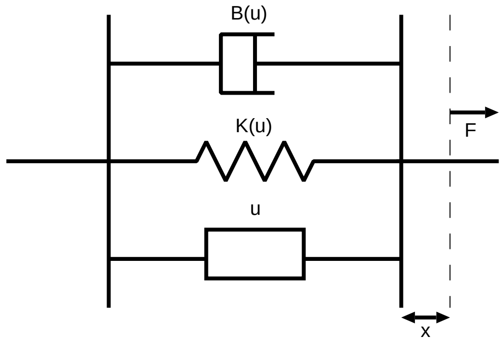

Fig. 2. Model of a muscle

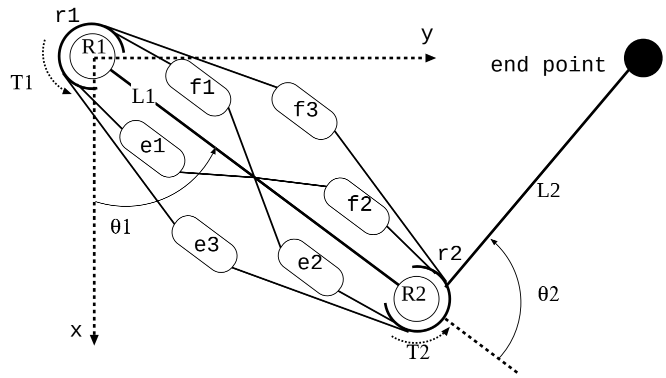

Fig. 3. Two joint link model with both mono-articular muscles and bi-articualr muscles

articular muscles and one antagonistic pair of bi-articular muscles. And they revealed that this model can explains recorded EMG patterns when human arms and legs output forces. [5][6]

II. MODELING OF MUSCULAR VISCOELASTICITY AND MUSCULAR ARRANGEMENTS

A. *viscoelastic muscle model*

Muscle has unique viscoelasticity. Animal Muscular model is shown in Fig. 2. According to Ito and Tsuji, muscular output force F is a function of contractile force u.[7]

$$F = u - K(u)x - B(u)\dot{x} = u - kux - bu\dot{x} \tag{1}$$

Here x is contracting length of the muscle and $\dot{x}$ is shortening velocity. k is elastic coefficient and b is viscosity coefficient. Contractile force u is only settled actively and others are passive elements. In other word u is assumed as activation level of muscle.

Muscles only generate forces when they shrink. Therefore muscles construct antagonistic pair to generate dual-directional force. We think summation and difference of contractile force for antagonistic pair.

$$M\ddot{x} = D - kSx - bS\dot{x} \tag{2}$$

Eq. 2 is dynamic equation of one-dimensional motion. D and S are difference and summation of contractile forces. M is mass of object. Summation of contractile forces controls elasticity and viscosity. Force exerted on object is generated by Difference of contractile forces and such passive forces.

B. *Two joint link model with bi-articular muscles*

In this paper we use simplified two joint link model shown in Fig. 3. In Fig. 3 e1 and f1 are a pair of antagonistic mono-articular muscles attached to joint R1. e2 and f2 are attached to R2. e3 and f3 are a pair of antagonistic bi-articular muscles attached both R1 and R2.

We define output forces of each muscle as F_{f1}, F_{e1}, F_{f2}, F_{e2}, F_{f3}, and F_{e3}. r_1 and r_2 are radii of R1 and R2. Joint moments T_1 and T_2 are as follows:

$$T_1 = (F_{f1} - F_{e1})r_1 + (F_{f3} - F_{e3})r_1$$

$$T_2 = (F_{f2} - F_{e2})r_2 + (F_{f3} - F_{e3})r_2 \tag{3}$$

The link model equipped both mono-articular muscles and bi-articular muscles like Fig. 3 can control output force and stiffness independently at its end point. When summations and differences of contractile forces are defined in each pair of antagonistic muscles, summations control stiffness and differences control force direction at end point. u_{f1}, u_{e1}, u_{f2}, u_{e2}, u_{f3} and u_{e3} are defined as contractile force in each muscle. Summations S_1, S_2, S_3 and differences D_1, D_2, D_3 are as follows:

$$\begin{aligned} S_1 &= u_{f1} + u_{e1} \quad , \quad D_1 = u_{f1} - u_{e1} \\ S_2 &= u_{f2} + u_{e2} \quad , \quad D_2 = u_{f2} - u_{e2} \\ S_3 &= u_{f3} + u_{e3} \quad , \quad D_3 = u_{f3} - u_{e3} \end{aligned} \tag{4}$$

under the following conditions:

$$|S_1| > |D_1| \, , \, |S_2| > |D_2| \, , \, |S_3| > |D_3|$$

Eq. (5) is derived from Eq. (3), Eq. (1) and Eq. (4). Joint torques T_1, T_2 are expressed using summations and differences of contractile forces.

$$\begin{aligned} T_1 &= r_1 D_1 - k r_1^2 \theta_1 S_1 - b r_1^2 \dot{\theta}_1 S_1 \\ &+ r_1 D_3 - k(r_1\theta_1 + r_2\theta_2) r_1 S_3 - b(r_1\dot{\theta}_1 + r_2\dot{\theta}_2) r_1 S_3 \\ T_2 &= r_2 D_2 - k r_2^2 \theta_2 S_2 - b r_2^2 \dot{\theta}_2 S_2 \\ &+ r_2 D_3 - k(r_1\theta_1 + r_2\theta_2) r_2 S_3 - b(r_1\dot{\theta}_1 + r_2\dot{\theta}_2) r_2 S_3 \end{aligned} \tag{5}$$

III. FF CONTROL ALGORITHM EMULATING MUSCULAR VISCOELASTICITY

When the contractile force of each muscle is settled, an equilibrium position is specified. Even robot arm takes any postures, it goes back to the equilibrium position. To change each contractile force we can drive the robot arm along the path of equilibrium position. At equilibrium joint angles θ_1, θ_2 are obtained from Eq. (5) in conditions of $T_1 = T_2 = 0$ and $r = r_1 = r_2$.

$$\begin{aligned} \theta_1 &= \frac{1}{kr} \frac{(D_1 + D_3)S_2 + (D_1 - D_2)S_3}{S_1 S_2 + S_2 S_3 + S_3 S_1} \\ \theta_2 &= \frac{1}{kr} \frac{(D_2 + D_3)S_1 - (D_1 - D_2)S_3}{S_1 S_2 + S_2 S_3 + S_3 S_1} \end{aligned} \tag{6}$$

In previous study[8], summation of contractile force and other parameters are determined using trial and error. We improve previous algorithm to determin such parameters by calcuration.

When expected path of the end point are given, we extract some intermediate point $X_m = [x_m, y_m]^T$ from the path. The subscript m denotes index of intermediate points. We derive desired joint angles $\theta^{\star}_{n,m}$ from intermediate points by Eq. (7). The subscript n denotes index of antagonistic pairs.

$$\begin{aligned}
\theta^{\star}_{1,m} &= \arctan(y_m, x_m) - \arctan(\sqrt{x_m^2 + y_m^2 - z_m^2}, z_m) \\
\theta^{\star}_{2,m} &= \arctan(y_m - l_1 \sin(\theta^{\star}_{1,m}), x_m - l_1 \cos(\theta^{\star}_{1,m})) - \theta^{\star}_{1,m} \\
\theta^{\star}_{3,m} &= \theta^{\star}_{1,m} + \theta^{\star}_{2,m}
\end{aligned} \tag{7}$$

where:

$$z_m = \frac{x_m^2 + y_m^2 + l_1^2 - l_2^2}{2l_1} \tag{8}$$

Eq. (9) is dynamic equation about each $\theta_{n,m}$. I_n is inertia around each joint.

$$I_n(\ddot{\theta_{n,m}}) = rD_{n,m} - kr^2\theta_{n,m}S_{n,m} - br^2\dot{\theta_{n,m}}S_{n,m} \tag{9}$$

In Eq. (10), we decide S_n in order that this system become critical damping.

$$S_{n,m} = \frac{4kI_n}{b^2r^2} \tag{10}$$

In this case, each joint become constant after settling time. Eq. (10) decide $D_{n,m}$ by this condition.

$$D_{n,m} = krS_{n,m}\theta^{\star}_{n,m+1} \tag{11}$$

$T_{n,m}$ is time length to force by each antagonistic pair. In Eq. (12), α is coefficient to decide smoothing.

$$T_{n,m} = \frac{\alpha I}{br^2 S_{n,m}} \tag{12}$$

When α is settled 1, $T_{n,m}$ equals rising time of this system. If intermediate points are settled enough densely, the arm can track the path smoothly.

IV. Simulation result of proposed method

Simulation model is shown in Fig. 4. Each link is a thin rod which has no thickness and width. Here l_1 and l_2 are lengths of L1 and L2, m_1 and m_2 are the masses, I_1 and I_2 are the inertia moments of links related to R_1 and R_2 , l_{g1} and l_{g2} are distances from each center of R_1 and R_2 to each gravity center of L_1 and L_2.

In Lagrangian mechanics the equation of motion are written in Eq. (13) T_1 and T_2 are joint torques. And θ_1 and θ_2 are joint angles. Gravitational effect are ignorable because robot arm moves only in horizontal plane.

$$\begin{pmatrix} T_1 \\ T_2 \end{pmatrix} = \begin{pmatrix} m_{11} & m_{12} \\ m_{21} & m_{22} \end{pmatrix} \begin{pmatrix} \ddot{\theta_1} \\ \ddot{\theta_2} \end{pmatrix} + \begin{pmatrix} h_{11} \\ h_{21} \end{pmatrix} \tag{13}$$

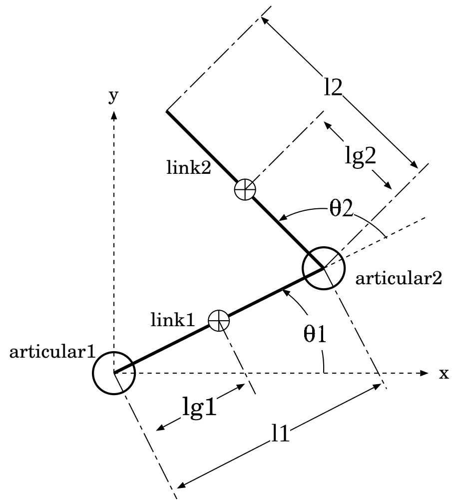

Fig. 4. Model for simulation

TABLE I
Parameters of simulation model

l_1	0.6[m]	l_2	0.6[m]
lg_1	0.3[m]	lg_2	0.3[m]
m_1	2.5[kg]	m_2	1.0[kg]
I_1	0.3[kg·m^2]	I_2	0.12[kg·m^2]
r_1	0.1[m]	r_1	0.1[m]
k	3.3[N/m]	b	1.0[N/m·s]

where:

$$\begin{aligned}
m_{11} &= I_1 + I_2 + 2m_2l_1l_{g2}\cos\theta_2 + m_2l_1^2 \\
m_{12} &= m_{21} = I_2 + m_2l_1l_{g2}\cos\theta_2, m_{22} = I_2 \\
h_{11} &= -m_2l_1l_{g2}\sin\theta_2(2\dot{\theta_1}\dot{\theta_2} + \dot{\theta_2}^2) \\
h_{21} &= m_2l_1l_{g2}\sin\theta_2\dot{\theta_1}^2
\end{aligned}$$

Simulation result is shown in Fig. 5 and parameters of arm model are shown in TABLE I. The exepected path is shown in Eq. (14).

$$(\frac{x - 0.3}{0.6})^2 + (\frac{y - 0.6}{0.2})^2 = 1 \tag{14}$$

We extract 40 intermediate point from this path and decide α as 1.0. This simulation shows that the arm can track expecting path smoothly.

Next we represent robustness of this algorithm. We inputs contractile forces equals to input forces of first simulation(Fig. 5). We assume that m_1 is 2.5 kg and m_1 is 1.0 kg. In this simulation, we change actual masses of each links and its result is shown in Fig. 6. Obviously the result shows amazing robustness of proposed feedforward method. When actual mass is twice as nominal mass, the arm can track expected path (central graph in bottom row of Fig. 6). This robustness is obtained by muscular viscoelasticity. When end point is displaced from expected path, muscular elasticity generates force to suppress its departure. Muscular viscocity stabilize its oscillation.

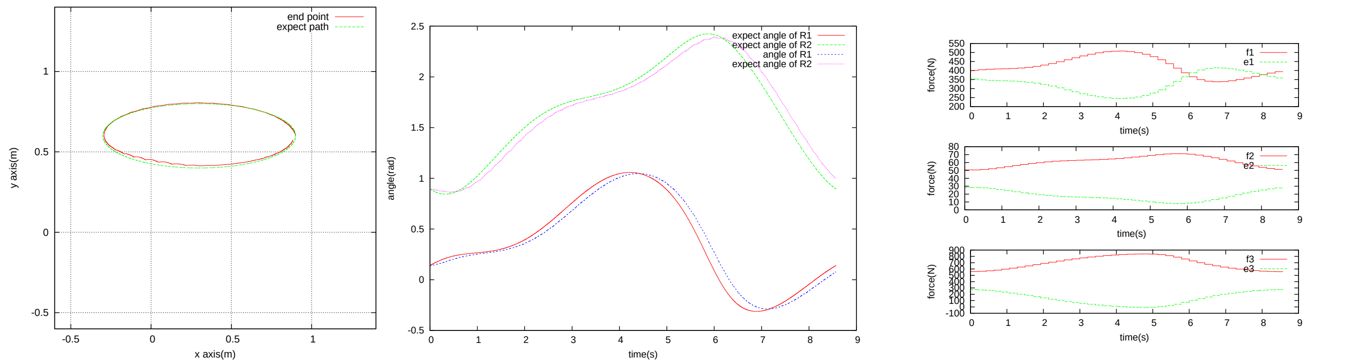

trajectory of endpoint   angles of each joint   contractile force of each muscle

Fig. 5. Simulation result of driving robot arm using muscular viscoelasticity
Left image is trajectory of endpoint. Center image is change of joint angles. Contractile forces of each muscle are indicated in right image.

However proposed algorithm has some improvable points. First it takes about 8.5 second to track around the expected path. This time depends on Eq. (12). When viscocity constant b is small, the algorithm generates big contractile forces. However too big contractile forces is undesirable. Thus b cannot be so small. To drive more quickly, it is necessary to weaken contractile forces in partial section. Next displacement from expected path is notable at a point that rate of change of traveling direction is big. Improvement of extracting intermediate points solve this problem. Also this improvement contributes for quick movement.

V. Experimental Robot arm equipped with bi-articular driving mechanism

We made robot arm based on bi-articular muscles principle. Fig. 7 is overview of this robot. It has two mono-articular driving mechanisms and one bi-articular driving mechanism. Mono-articular driving mechanism is implementation of antagonistic mono-articular muscle pair. Bi-articular driving mechanism is implementation of antagonistic bi-articular muscle pair.

In this robot, each driving mechanism use electric rotary motors. Muscular viscoelasticity is actualized by a nonlinear feedback control block (Fig. 8). In this block diagram, $\otimes$ means multiplication of inputs. Each joint angles are detected by rotary encoders to calculated elasticity and viscosity. Furthermore current bi-articular driving mechanism is incomplete. We compensate this problem using shoulder side mono-articular driving mechanism.

Fig. 9 is a photo of mechanical part of the robot. Whole control diagram is shown in Fig. 10. In this diagram, contractile forces generater is implementation of our proposed algorithm. Generating contractile forces is transmitted to each antagonistic muscle module. Our robot has only incomplete bi-articular driving mechanisms, therefore force distributor works as a compensator. R1 side output force of bi-articular driving mechanism was generate by R1 side mono-articular driving mechanism actually. Eq. (15) is

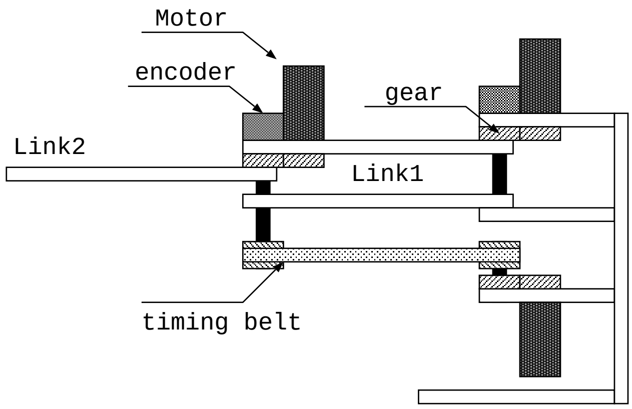

Fig. 7. Overview of our robot arm

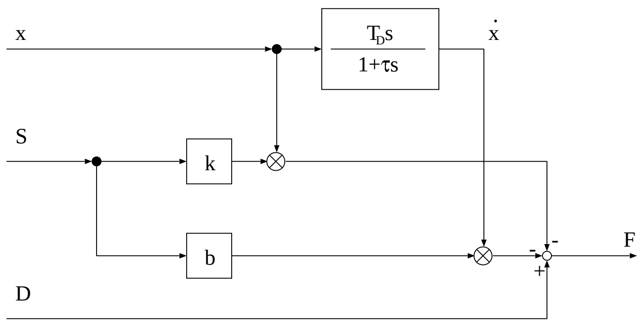

Fig. 8. Control diagram to generate force of antagonistic pair

shown this compensation.

$$\begin{pmatrix} i_1^* \\ i_2^* \\ i_3^* \end{pmatrix} = \begin{pmatrix} K_i & 0 & K_i \\ 0 & K_i & 0 \\ 0 & 0 & K_i \end{pmatrix} \begin{pmatrix} F_1^* \\ F_2^* \\ F_3^* \end{pmatrix} \tag{15}$$

Each motor has a current controller and is driven by PWM. The robot arm is drived with feedback control as is clear from whole diagram. We use feedback control only to mimic animal characteristic. Ideal arm with muscular arrangements and viscoelasticity is controlled by feedforward.

Table II shows major parameters of robot. And Table

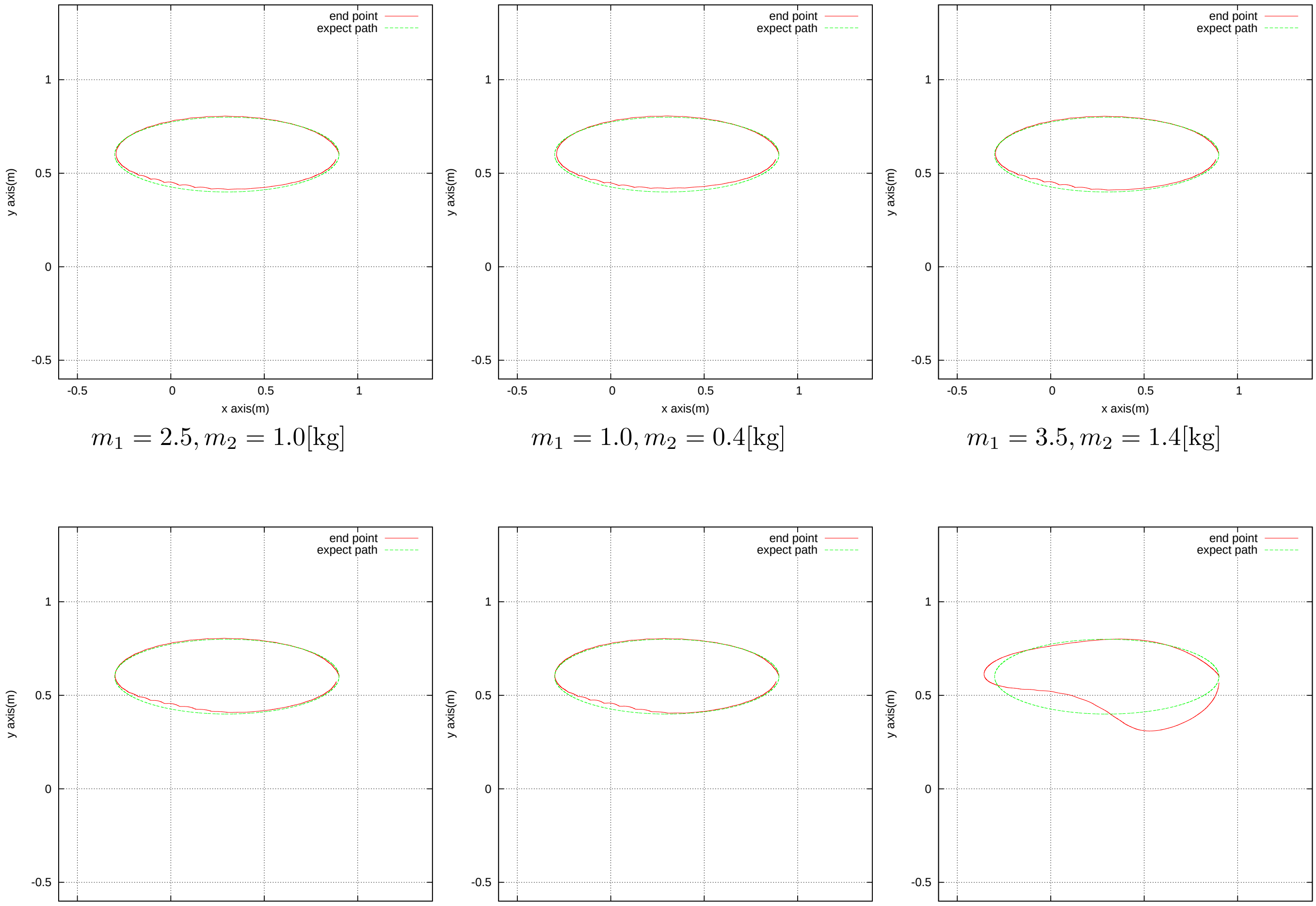

$m_1 = 2.5, m_2 = 1.0$[kg] $m_1 = 1.0, m_2 = 0.4$[kg] $m_1 = 3.5, m_2 = 1.4$[kg]

$m_1 = 2.5, m_2 = 2.5$[kg] $m_1 = 5.0, m_2 = 2.0$[kg] $m_1 = 25.0, m_2 = 10.0$[kg]

Fig. 6. Simulation result of changing mass of each link

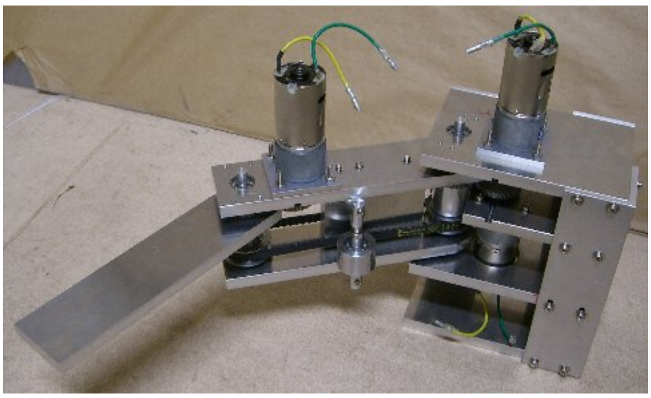

Fig. 9. A photo of actual robot arm

TABLE II

MAJOR PARAMETERS OF ROBOT ARM

Total hight	about 250[mm]
Total length	about 500[mm]
Link1(upper,bottom)	200×50×10mm 270g
Link2	200×50×10mm 270g
Motors	TAMIYA(540K75)
Encoders	OMRON(E6H-CWZ6C)
Current sensor	U_RD(HCS-20-SC-A-2.5)

III shows major parts of controller.

VI. Conclusion and future works

In this paper we described the new feedforward algorithm for robot arm based on bi-articular muscle principle. This algorithm use muscular viscoelasticity effectively to realize path tracking. The algorithm also has remarkable ability of disturbances suppression in spite of feedforward control. We verified this algorithm by simulation and represent its robustness for model disturbance.

For the experiment we developed novel robot arm. It has bi-articular driving mechanism and emulate muscular viscoelasticity. We will experiment for verification of above algorithm using this robot arm.

References

[1] G. J. van Ingen Shenau, M. F. Bobbert and R. H. Rozendal, “The unique action of bi-articular muscles in complex move-

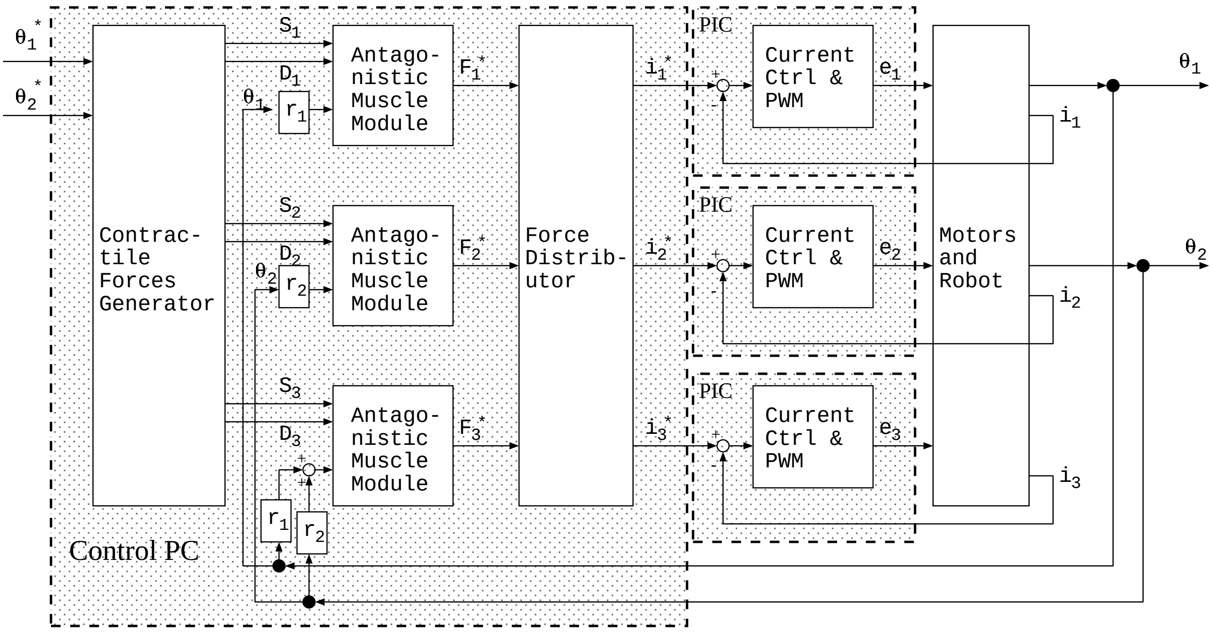

Fig. 10. Whole control diagram

TABLE III
PARTS OF CONTROLLER

CPU board	Advantech (PCM-9371F-J0A1)
Counter board	TAC(T104-C160)
AD-DA board	TAC(T104-ADA)
Current Controller and PWM	Microchip(16F877)
H-bridge	Toshiba(2SK2312)
Gate driver	Nihon Pulse(FDM2B) Toshiba(2SK1484)

ments", Journal of Anatomy, 155, pp. 1-5, 1987

[2] Neville Hogan, "Adaptive Control of Mechanical Impedance by Coactivation of Antagonist Muscles", IEEE Transactions on Automatic Control, vol.AC-29, No.8, pp. 681-690, 1984

[3] Neville Hogan, "On the stability of Manipulators Performing Contact Tasks", IEEE Journal of Robotics and Automation, Vol. 4, No. 6, pp. 677-686, 1988

[4] F. A. Mussa Ivaldi, N. Hogan and E. Bizzi, "Neural, Mechanical, and Geometric Factors Subserving Arm Posture in Humans", The Journal of Neuroscience, Vol. 5, No. 10, pp. 2732-2743, 1985

[5] Mizuyori Kumamoto, Toru Oshima, Tomohisa Yamamoto, "Control properties induced by existence of antagonistic pairs of bi-articular muscles -Mechanical engineering model analyses", Human Movement Science 13, pp. 611-634, 1994

[6] Toru Oshima, Tomohiko Fujikawa and Mizuyori Kumamoto, "Mechanical Properties of Robot Arm Operated with Muscle Coordinate System Consisted of Bi-articular muscles and Mono-articular Muscles - Muscle Contractile Forces and Viscoelastic Properties of Robot Arm -", Journal of The Japan Society for Precision Engineering, vol. 66, No. 1, pp. 141-146, 2000.

[7] K. Ito and T. Tsuji, "The bilinear characteristics of Muscle-Skeletomotor system and the application to prosthesis control", The Transactions of the Electrical Engineers of Japan 105-C(10), pp. 201-208, 1985

[8] Kengo Yoshida, Naoki Hata, Toshiyuki Uchida, Yoichi Hori, "A Novel Design and Realization of Robot Arm Based on the Principle of Bi-articular Muscles", Proc. IEEE International Conference on Industrial Technology (ICIT), 2006. 12